

# Oxidative Damage in MauG: Implications for the Control of High-Valent Iron Species and Radical Propagation Pathways

Erik T. Yukl,<sup>\*,†</sup> Heather R. Williamson,<sup>‡</sup> LeeAnn Higgins,<sup>‡</sup> Victor L. Davidson,<sup>§</sup> and Carrie M. Wilmot<sup>\*,‡</sup>

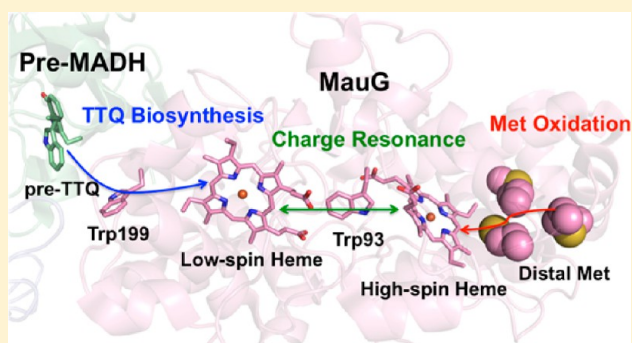
<sup>†</sup>Department of Chemistry and Biochemistry, New Mexico State University, Las Cruces, New Mexico 88003, United States

<sup>‡</sup>Department of Biochemistry, Molecular Biology and Biophysics, University of Minnesota, Minneapolis, Minnesota 55455, United States

<sup>§</sup>Burnett School of Biomedical Sciences, College of Medicine, University of Central Florida, Orlando, Florida 32827, United States

## S Supporting Information

**ABSTRACT:** The di-heme enzyme MauG catalyzes the oxidative biosynthesis of a tryptophan tryptophylquinone cofactor on a precursor of the enzyme methylamine dehydrogenase (preMADH). Reaction of H<sub>2</sub>O<sub>2</sub> with the diferric form of MauG, or reaction of O<sub>2</sub> with diferrous MauG, forms the catalytic intermediate known as bis-Fe(IV), which acts as the key oxidant during turnover. The site of substrate oxidation is more than 40 Å from the high-spin heme iron where H<sub>2</sub>O<sub>2</sub> initially reacts, and catalysis relies on radical hopping through an interfacial residue, Trp199 of MauG. In the absence of preMADH, the bis-Fe(IV) intermediate is remarkably stable, but repeated exposure to H<sub>2</sub>O<sub>2</sub> results in suicide inactivation. Using mass spectrometry, we show that this process involves the oxidation of three Met residues (108, 114, and 116) near the high-spin heme through ancillary electron transfer pathways engaged in the absence of substrate. The mutation of a conserved Pro107 in the distal pocket of the high-spin heme results in a dramatic increase in the level of oxidation of these Met residues. These results illustrate structural mechanisms by which MauG controls reaction with its high-valent heme cofactor and limits uncontrolled oxidation of protein residues and loss of catalytic activity. The conservation of Met residues near the high-spin heme among MauG homologues from different organisms suggests that eventual deactivation of MauG may function in a biological context. That is, methionine oxidation may represent a protective mechanism that prevents the generation of reactive oxygen species by MauG in the absence of preMADH.



Many enzymes utilize metals or metal-containing cofactors capable of forming high-valent species to catalyze difficult oxidative reactions. One well-known example of this comes from the cytochromes P450 that use a heme cofactor to activate molecular oxygen, generating an Fe(IV)=O heme with an associated cation radical centered either on the heme macrocycle (compound I) or on a nearby amino acid (compound ES).<sup>1</sup> The utilization of amino acid radicals, which are often generated by a high-valent metallo cofactor,<sup>2</sup> is also widespread in biological catalysis. In a process known as hole “hopping”, transient amino acid radicals allow efficient electron transfer across distances longer than those supported by electron tunneling alone.<sup>3</sup> In this way, a substrate can be oxidized at a site many angstroms from where the oxidative potential is initially generated. For example, the class Ia ribonucleotide reductases (RNR) utilize a di-iron cofactor to generate a stable radical on a nearby Tyr residue. This radical can then reversibly generate a transient catalytic Cys radical ~35 Å away across a protein interface through a hopping mechanism involving transient Tyr radicals between the two sites.<sup>4</sup>

Although high-valent cofactor intermediates and amino acid radicals are central to many essential cellular processes, they are also potentially dangerous to the cell. By nature, both are highly reactive and must be carefully controlled to prevent the generation of harmful reactive oxygen species (ROS) and oxidation of unintended substrates. Underscoring the importance of such regulation is the observation that elevated ROS levels and oxidative modifications to proteins are implicated in a wide range of disease states, as well as the natural process of aging.<sup>5</sup> Thus, it is of interest to determine how proteins are able to stabilize and control high-valent species and amino acid radicals to prevent unwanted oxidation events.

The di-heme *c* enzyme MauG catalyzes the oxidative modification of two tryptophan residues on a precursor of methylamine dehydrogenase (preMADH) to generate the tryptophan tryptophylquinone (TTQ) cofactor<sup>6,7</sup> (Figure 1). The catalytic species is generated by reaction of diferric MauG with H<sub>2</sub>O<sub>2</sub> to form a high-valent intermediate termed bis-

Received: October 22, 2013

Revised: December 5, 2013

Published: December 9, 2013

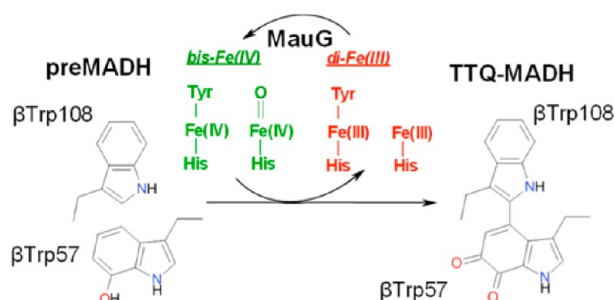


**Figure 1.** Schematic representation of the reaction of MauG with  $\text{H}_2\text{O}_2$  to generate the bis-Fe(IV) intermediate and its reaction with preMADH to yield the TTQ cofactor.

Fe(IV).<sup>8</sup> In this species, both hemes are oxidized to the Fe(IV) state; however, the formerly high-spin heme becomes an Fe(IV)=O (ferryl) species, while the low-spin heme retains its Tyr and His ligands (Figure 1). Bis-Fe(IV) MauG provides the oxidizing power required to extract electrons from the protein substrate, preMADH, during TTQ biosynthesis. A conserved Trp93 residue sits between the two MauG hemes, and its rapid, reversible oxidation is responsible for the charge resonance stabilization of the high-valent intermediate.<sup>9</sup> Although bis-Fe(IV) is the dominant resonance structure, compound ES and compound I-like resonance structures make small contributions to the ensemble of two-electron-oxidized species. The electron transfer pathway from the preMADH substrate to the MauG bis-Fe(IV) hemes has been characterized and shown to involve the transient oxidation of Trp199 of MauG that lies at the interface with preMADH.<sup>10,11</sup> Mutation of this residue to Phe, which cannot be oxidized by the bis-Fe(IV) hemes, completely abrogates the activity toward preMADH. Thus, completion of TTQ biosynthesis by MauG requires the formation of a high-valent intermediate [bis-Fe(IV)] involving an amino acid radical (Trp93), as well as an additional tryptophan radical (Trp199) involved in hole hopping.

Although bis-Fe(IV) MauG reacts rapidly with preMADH, it is remarkably stable in the absence of substrate, decaying back to the di-Fe(III) state over the course of minutes.<sup>12</sup> Despite this stability, MauG has been shown to undergo suicide inactivation with  $\text{H}_2\text{O}_2$  in the absence of preMADH.<sup>13</sup> Because only a small amount of heme degradation was observed, it was postulated that the loss of activity was most likely caused by the oxidation of a critical amino acid. The subsequent observation of a +16 species by electrospray ionization mass spectrometry (ESI-MS) of intact MauG incubated with  $\text{H}_2\text{O}_2$  is consistent with that hypothesis.<sup>14</sup> In this study, we further investigate the process of oxidative modification in MauG using mass spectrometry and UV–visible–near-infrared (UV–vis–NIR) absorption spectroscopy. Results for the WT protein compared with those of several variants of MauG elucidate general mechanisms that prevent uncontrolled reaction of the potent bis-Fe(IV) oxidant.

## MATERIALS AND METHODS

**Protein Expression and Purification.** Recombinant MauG was expressed in *Paracoccus denitrificans* and purified by Ni affinity chromatography as described previously.<sup>15</sup> Mutants of Pro107,<sup>14</sup> Glu113,<sup>16</sup> and Trp199<sup>11</sup> were generated by site-directed mutagenesis and expressed and purified from *P. denitrificans* as for the WT enzyme.

**UV–Visible–Near-Infrared Absorption Spectroscopy.** Concentrations of MauG and  $\text{H}_2\text{O}_2$  were calculated using

extinction coefficients  $\epsilon_{405}$  ( $208000 \text{ M}^{-1} \text{ cm}^{-1}$ )<sup>17</sup> and  $\epsilon_{240}$  ( $43.6 \text{ M}^{-1} \text{ cm}^{-1}$ ),<sup>18</sup> respectively. MauG was prepared in 10 mM potassium phosphate (pH 7.5) in a quartz cuvette at a concentration of  $5.0 \mu\text{M}$  and equilibrated to  $25^\circ\text{C}$  in a temperature-controlled cuvette holder. Stoichiometric  $\text{H}_2\text{O}_2$  was added from a concentrated stock solution, and the initial formation of bis-Fe(IV) MauG was confirmed spectroscopically. Spectra monitoring the subsequent decay of the bis-Fe(IV) species back to the diferric enzyme were recorded until no further changes were observed (typically  $\sim 1 \text{ h}$ ). This process was repeated three times, at which point no further reaction with  $\text{H}_2\text{O}_2$  could be detected. All spectra were recorded on a Cary 50 UV–vis spectrophotometer (Varian).

**Whole Protein Mass Spectrometry.** For reaction with stoichiometric  $\text{H}_2\text{O}_2$ , reaction mixtures were prepared in a final volume of  $80 \mu\text{L}$  and contained  $20 \mu\text{M}$  MauG and  $100 \mu\text{M}$  diethylenetriaminepentaacetic acid (DTPA) in 10 mM potassium phosphate (pH 7.5). Reactions were initiated by the addition of  $\text{H}_2\text{O}_2$  to a final concentration of  $20 \mu\text{M}$  and mixtures incubated for 1 h at room temperature. A  $20 \mu\text{L}$  aliquot was then removed, and 250 units of bovine liver catalase (Sigma) was added to remove residual  $\text{H}_2\text{O}_2$ . This process was repeated three times. For reaction with excess  $\text{H}_2\text{O}_2$ , reaction mixtures were prepared in a final volume of  $20 \mu\text{L}$  and contained  $20 \mu\text{M}$  MauG and  $100 \mu\text{M}$  diethylenetriaminepentaacetic acid (DTPA) in 10 mM potassium phosphate (pH 7.5). Reactions were initiated by the addition of  $\text{H}_2\text{O}_2$  to a final concentration of  $200 \mu\text{M}$  and mixtures incubated for 1 h at room temperature. Two hundred fifty units of bovine liver catalase (Sigma) was then added to remove residual  $\text{H}_2\text{O}_2$ . Control samples were prepared under identical conditions in the absence of  $\text{H}_2\text{O}_2$ . Half of the control and reaction mixtures were set aside for trypsin digest and liquid chromatography with tandem mass spectrometry (LC–MS/MS) (see below). The remaining samples were desalted and exchanged into a 75:25 (v/v) acetonitrile/water mixture with 0.1% formic acid using C4 resin ZipTip pipet tips (Millipore) prior to introduction into the mass spectrometer. Data were acquired on a QSTAR XL (AB Sciex, Framingham, MA) quadrupole time-of-flight (TOF) mass spectrometer with the IonSpray electrospray ionization (ESI) source as described previously.<sup>14</sup>

**Proteolysis and Liquid Chromatography with Tandem Mass Spectrometry.** Aliquots of the control and  $\text{H}_2\text{O}_2$ -treated MauG samples described above were diluted 2-fold to  $10 \mu\text{L}$  with 100 mM ammonium bicarbonate (pH 8.5). Proteomics grade trypsin (Agilent) was added at a mass ratio of 1:50 to MauG and incubated at  $37^\circ\text{C}$  overnight. Reactions were quenched by the addition of formic acid to a final concentration of 0.1%. Samples were desalted and exchanged into an 80:20 acetonitrile/water mixture with 0.1% formic acid using a STAGE tip desalting procedure.<sup>19</sup> Samples were evaporated to dryness and dissolved in a 2:98 acetonitrile/water mixture with 0.1% trifluoroacetic acid for analysis by LC–MS/MS on a LTQ Orbitrap Velos (Thermo Scientific) as described previously.<sup>20</sup> ProteinPilot version 4.2 (AB Sciex), which uses the Paragon scoring algorithm<sup>21</sup> and the ProGroup protein grouping algorithm, was used for tandem mass spectrometry data searching against a *P. denitrificans* database from NCBI Reference Sequence, combined with the common contaminants database from <http://www.thegpm.org/crap/>. Search parameters were as follows: trypsin; instrument Orbi MS (1–3 ppm) Orbi MS/MS; biological modifications and amino acid substitution ID focus; thorough search effort; and

False Discovery Rate analysis.<sup>22</sup> After identification of possible modifications, MS/MS data were manually inspected using Xcalibur version 2.1.0 for validation of search results and match integrity.

### Offline High-Performance Liquid Chromatography (HPLC) and Mass Spectrometry of Heme Peptides.

Twenty microliters each of control and H<sub>2</sub>O<sub>2</sub>-treated samples were made up as described above, except at concentrations of 50  $\mu$ M MauG and 500  $\mu$ M H<sub>2</sub>O<sub>2</sub>. After being incubated at room temperature for 1 h, catalase was added, and the samples were diluted to 50  $\mu$ L in 50 mM ammonium bicarbonate (pH 7.5). Proteomics grade trypsin was added at a final trypsin:MauG mass ratio of 1:50, and the samples were incubated overnight at 37 °C. Formic acid was added to a final concentration of 1%, and samples were filtered through 0.22  $\mu$ m centrifugal spin filters (Millipore) prior to manual injection into a 50  $\mu$ L sample loop. Samples were loaded onto a C4 resin column (Phenomenex) pre-equilibrated with a 5:95 (v/v) acetonitrile/water mixture with 0.1% formic acid at a rate of 1 mL/min. The column was washed with the mixture described above for 3 min, at which point a linear gradient was applied from 5 to 50% acetonitrile at a flow rate of 1 mL/min over 27 min. Fractions were collected every 30 s, and the elution profile was monitored by a dual-channel detector at 215 and 370 nm. Fractions containing the heme peptides were evaporated to dryness and reconstituted in 30  $\mu$ L of a 50:50 (v/v) acetonitrile/water mixture with 0.1% formic acid, and 10  $\mu$ L was directly injected into the QSTAR XL (AB Sciex) instrument and analyzed as described above. After peptides of interest had been identified, another 10  $\mu$ L aliquot was injected and the *m/z* of interest subjected to MS/MS. Time-of-flight (TOF) MS/MS spectra were recorded from *m/z* 100 to 1100 for approximately 5 min with a 1 s accumulation time. The acquisition software was Analyst QS version 1.0 (AB Sciex).

## RESULTS

### Oxidative Modification of MauG Correlates with Loss of Function.

It was previously shown that four cycles of bis-Fe(IV) formation and decay in the absence of substrate were sufficient to completely eliminate MauG catalytic activity.<sup>13</sup> Here, UV–vis–NIR absorption spectroscopy was used to track this process. Upon addition of stoichiometric H<sub>2</sub>O<sub>2</sub>, features characteristic of the bis-Fe(IV) intermediate were observed. These include a decrease in absorbance and a red shift of the Soret band, a sharpening and increase in absorbance in the 500–600 nm region (the  $\alpha/\beta$  bands),<sup>12</sup> and a broad feature in the NIR region at 950 nm.<sup>9</sup> The characteristic bis-Fe(IV) spectrum then slowly decayed to a spectrum similar but not identical to the initial di-Fe(III) spectrum (Figure 2A). After the decay process had reached completion and no further changes had been observed ( $\sim$ 1 h), a second stoichiometric addition of H<sub>2</sub>O<sub>2</sub> was made. Features consistent with bis-Fe(IV) formation were again observed, but in a reduced yield. Quantifying the relative concentration of bis-Fe(IV) by its absorbance at 950 nm suggests that only  $\sim$ 50% of the intermediate is re-formed upon the second addition of H<sub>2</sub>O<sub>2</sub>. This trend continued until no changes were observed upon the fourth addition of stoichiometric H<sub>2</sub>O<sub>2</sub> (Figure 2B). The loss of the ability of MauG to form the bis-Fe(IV) species closely matches the loss of catalytic activity reported previously,<sup>13</sup> suggesting a causal relationship. The di-Fe(III) state to which bis-Fe(IV) MauG decayed also continued to change over this

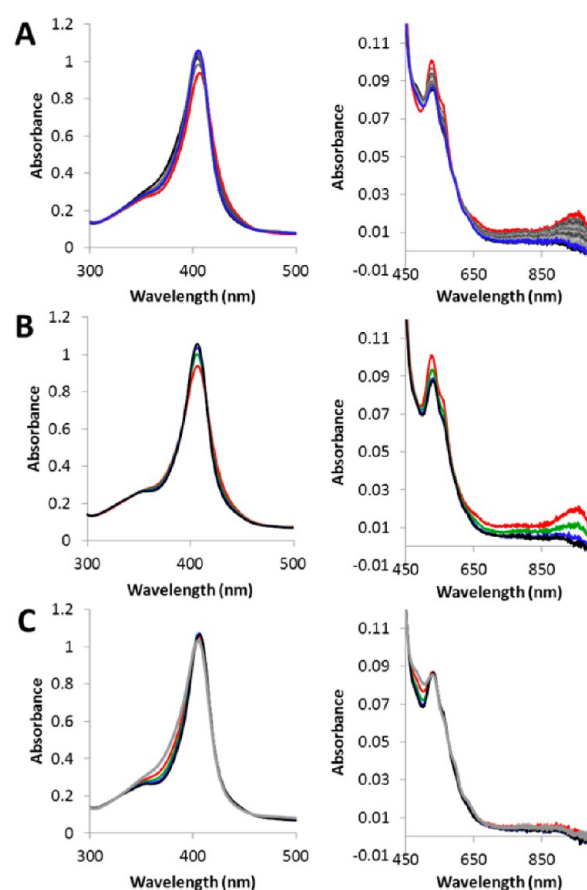


**Figure 2.** UV–vis–NIR spectra. (A) Reaction of di-Fe(III) WT MauG (black) with 1 equiv of H<sub>2</sub>O<sub>2</sub> to form bis-Fe(IV) (red) followed by its decay (grayscale) to a final resting state (blue). (B) Decreasing yields of bis-Fe(IV) immediately after addition of 1 (red), 2 (green), 3 (blue), and 4 equiv (black) of H<sub>2</sub>O<sub>2</sub> in cycles of stoichiometric additions of H<sub>2</sub>O<sub>2</sub> and bis-Fe(IV) decay. (C) Comparison of the initial di-Fe(III) MauG (gray) to the decay products formed after one (red), two (green), three (blue), and four (black) cycles of stoichiometric additions of H<sub>2</sub>O<sub>2</sub> and bis-Fe(IV) decay.

interval (Figure 2C), indicative of a change in the heme environment for the resting state.

To determine whether oxidative modifications to MauG correlated with the observed loss of H<sub>2</sub>O<sub>2</sub> reactivity, aliquots from a sample of WT MauG were removed 1 h after each addition of stoichiometric H<sub>2</sub>O<sub>2</sub>, quenched with catalase, and analyzed by whole protein ESI-MS (Figure 3A). After the first addition of H<sub>2</sub>O<sub>2</sub>, a significant proportion of a +16 adduct appears, which increases after the second addition. The third and fourth cycles result in an increasing proportion of a +32 adduct, the appearance of a +48 adduct, and the near disappearance of the native protein. These data show that oxidative modification accompanies the loss of H<sub>2</sub>O<sub>2</sub> reactivity and catalytic activity in MauG.

To localize the observed modifications to H<sub>2</sub>O<sub>2</sub>-treated MauG, the samples described above were digested with trypsin and subjected to LC–MS/MS. The sequence coverage was  $\geq$ 72% for all samples at a level of confidence of 99% (a Paragon scoring parameter). The MS/MS data were searched using ProteinPilot (AB Sciex) with parameters set to identify biological modifications. Among the peptide modifications identified were multiple oxidations to the Q102–R119 peptide as a result of H<sub>2</sub>O<sub>2</sub> treatment, which was validated by manual



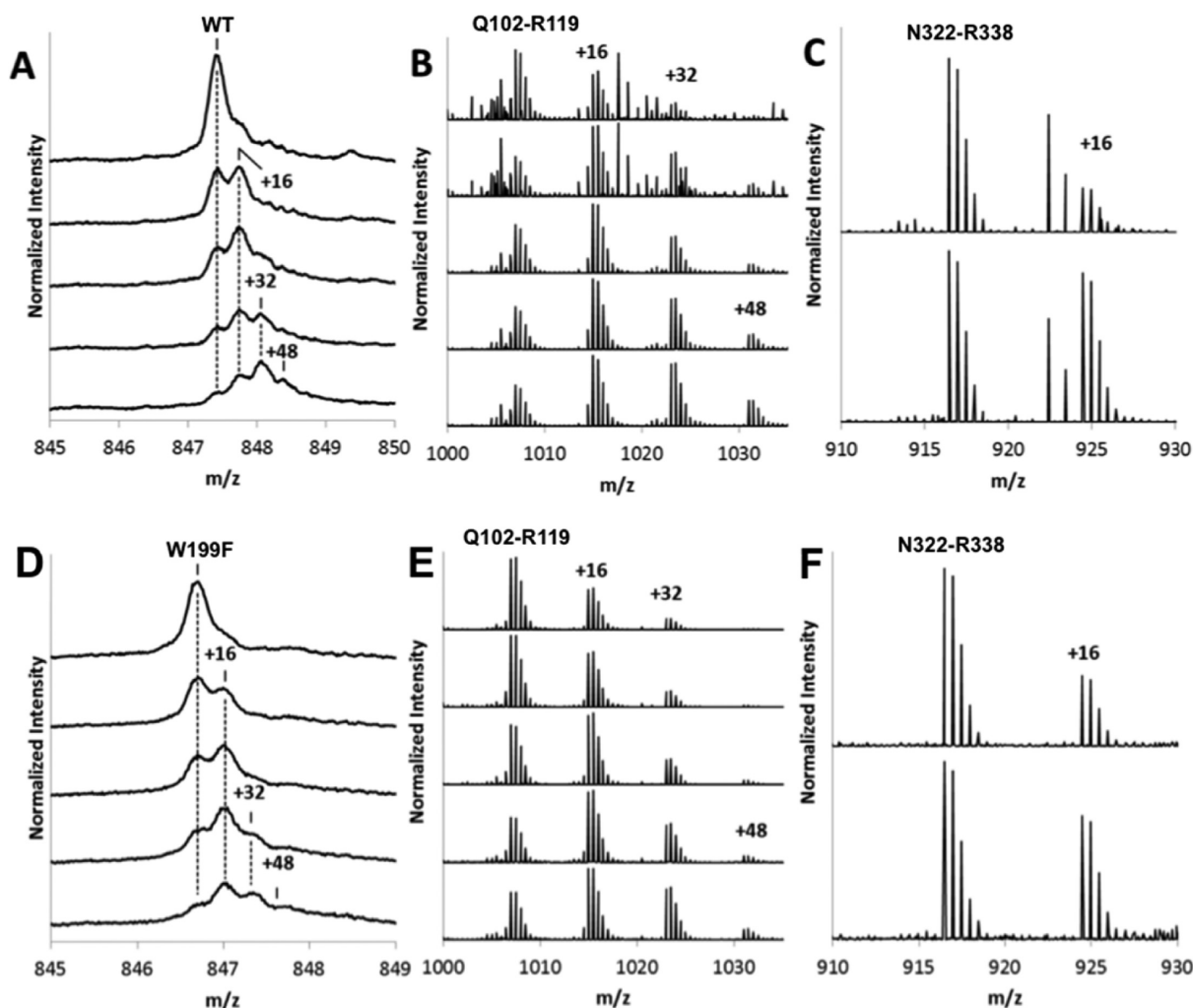


**Figure 3.** H<sub>2</sub>O<sub>2</sub>-induced oxidation of WT (A–C) and W199F (D–F) MauG. (A and D) Whole protein mass spectra highlighting the +50 charge peak of MauG after zero to four sequential cycles of addition of stoichiometric H<sub>2</sub>O<sub>2</sub> and bis-Fe(IV) decay (increasing additions going downward). (B and E) LC–MS data showing the +2 charge state of the Q102–R119 peptide after zero to four sequential cycles of addition of stoichiometric H<sub>2</sub>O<sub>2</sub> and bis-Fe(IV) decay (increasing additions going downward). (C and F) LC–MS data showing the +2 charge state of the N322–R338 peptide after zero (top) and four (bottom) sequential additions of stoichiometric H<sub>2</sub>O<sub>2</sub> and bis-Fe(IV) decay. The numbers represent the increase in the total mass of the peptide relative to that of the unmodified peptide.

inspection of the data (Figure 3B). The increasing level of oxidation with additions of increasing amounts of H<sub>2</sub>O<sub>2</sub> at the peptide level correlates with the whole protein data, which collectively support the appearance of a +16 adduct followed by a +32 adduct and a small amount of a +48 adduct. Tandem mass spectra of the oxidized species demonstrate that the initial oxidation preferentially occurs at Met108, followed by Met114 and Met116 (Table 1).

Oxidation of a second peptide, N322–R338 (Figure 3C), was also identified at Met333 in samples treated with multiple sequential additions of stoichiometric H<sub>2</sub>O<sub>2</sub>. This modification was interesting in that Met333 is adjacent to Trp199 in the crystal structure of the MauG–preMADH complex with the nearest approach between residues being 3.1 Å.<sup>23</sup> Thus, oxidation of Met333 may be due to radical hopping through Trp199 to the bis-Fe(IV) MauG hemes. To test the radical hopping hypothesis, a W199F variant of MauG was subjected to an identical H<sub>2</sub>O<sub>2</sub> treatment and analyzed by MS. The results were very similar to the results for the WT protein (Figure 3D–F). Most importantly, Met333 is oxidized upon repeated exposure to stoichiometric H<sub>2</sub>O<sub>2</sub> as it was in the WT protein,

which suggests that oxidation of this residue does not require an intact radical hopping pathway through Trp199. Rather, oxidation may be a result of direct reaction with H<sub>2</sub>O<sub>2</sub> because, on the basis of the crystal structure,<sup>23</sup> this residue would be surface-exposed in the absence of preMADH.

**Oxidation of MauG Variants of High-Spin Heme Distal Residues.** Oxidation of the E113Q variant of MauG was analyzed to confirm that oxidation of Met108, Met114, and Met116 requires efficient formation of bis-Fe(IV), while oxidation of Met333 is the result of direct, nonspecific reaction with H<sub>2</sub>O<sub>2</sub>. Glu113 is proposed to act as a general base in the high-spin heme active site, promoting O–O bond cleavage and the formation of the bis-Fe(IV) intermediate.<sup>24</sup> The E113Q mutation does not alter the structure of MauG, but it decreases the rate of reaction with H<sub>2</sub>O<sub>2</sub> and alters the distribution of high-valent resonance structures such that bis-Fe(IV) is no longer the predominant species and activity toward preMADH is lost.<sup>16</sup> Upon incubation of E113Q MauG with a 10-fold excess of H<sub>2</sub>O<sub>2</sub>, no significant oxidation was detected by whole protein ESI-MS (Figure S1D of the Supporting Information), nor was any increased level of oxidation of the Q102–R119

**Table 1. Masses and Sites of Oxidative Modifications of the Q102–R119 Tryptic Peptide in WT, P107V, and P107S MauG upon Incubation with a 10-fold Excess of H<sub>2</sub>O<sub>2</sub>**

peptide	calculated mono <sup>a</sup> [M + 2H] <sup>2+</sup>	observed mono <sup>a</sup> [M + 2H] <sup>2+</sup>	modification
WT Q102–R119 + 16	1014.97	1014.97	OxMet108
WT Q102–R119 + 32	1022.96	1022.97	OxMet108, OxMet114
WT Q102–R119 + 48	1030.97	1030.96	OxMet108, OxMet114, OxMet116
P107V Q102–R119 + 16	1015.97	1015.98	OxMet108
P107V Q102–R119 + 32	1023.97	1023.98	OxMet108, OxMet114
P107V Q102–R119 + 48	1031.97	1031.97	OxMet108, OxMet114, OxMet116
P107V Q102–R119 + 64	1039.97	1039.97	DiOxMet108, OxMet114, OxMet116
P107V Q102–R119 + 80	1047.96	1047.97	DiOxMet108, OxMet114, DiOxMet116
P107S Q102–R119 + 48	1025.95	1025.94	OxMet108, OxMet114, OxMet116
P107S Q102–R119 + 64	1033.95	1033.95	DiOxMet108, OxMet114, OxMet116
P107S Q102–R119 + 80	1041.94	1041.95	DiOxMet108, OxMet114, DiOxMet116
P107S Q102–R119 + 96	1049.93	1049.95	DiOxMet108, DiOxMet114, DiOxMet116

<sup>a</sup>Monoisotopic *m/z* values are for the +2 charge states.

peptide observed (Figure S2A of the Supporting Information). Conversely, LC–MS/MS data showed an increased level of oxidation of Met333 in the presence of H<sub>2</sub>O<sub>2</sub> (Figure S2B of the Supporting Information), demonstrating that oxidation of Met108, Met114, and Met116 of MauG requires the efficient formation of bis-Fe(IV) and is not a simply a result of direct oxidation by H<sub>2</sub>O<sub>2</sub>.

In contrast to the E113Q mutant, mutation of high-spin heme distal residue Pro107 to Val or Ser results in a dramatically increased susceptibility to oxidation upon incubation with a 10-fold excess of H<sub>2</sub>O<sub>2</sub> as demonstrated by whole protein ESI-MS<sup>14</sup> (Figure S1 of the Supporting Information). Given their hyperoxidation phenotype, it was of interest to determine the sites of oxidation in the Pro107 variants. Therefore, control and H<sub>2</sub>O<sub>2</sub>-treated WT, P107V, and P107S MauG were digested with trypsin and subjected to LC–MS/MS as described above. The sequence coverage for the mutant proteins was similar to the coverage obtained for the WT experiments. Like the WT, oxidative modifications of the Q102–R119 peptide were identified in P107S and P107V MauG upon treatment with H<sub>2</sub>O<sub>2</sub> (Figure 4). However, the degree of oxidation was significantly increased in these mutants, consistent with the whole protein ESI-MS (Figure S1 of the Supporting Information). Namely, some of the unmodified peptide is retained in H<sub>2</sub>O<sub>2</sub>-treated P107V MauG, but there is also a series of multiply oxidized species formed. In H<sub>2</sub>O<sub>2</sub>-treated P107S MauG, the unmodified peptide is completely absent and a series of even more oxidized species is observed. The precise positions of oxidative modifications on this peptide were determined by acquiring MS/MS spectra for each species. The results are summarized in Table 1 and show that all modifications can be localized to the same three Met residues

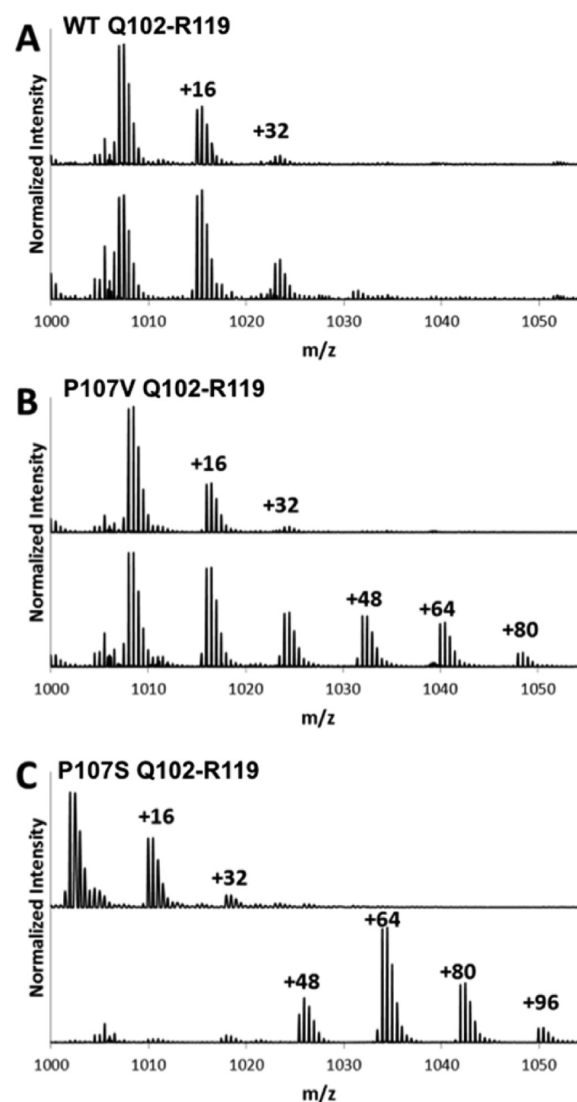


**Figure 4.** LC–MS data showing the +2 charge state of the Q102–R119 peptide of WT (A), P107V (B), and P107S (C) before (top trace) and after (bottom trace) incubation with a 10-fold excess of H<sub>2</sub>O<sub>2</sub>. The numbers represent the increase in the total mass of the peptide relative to that of the unmodified peptide.

oxidized in the WT protein. For peptides in which more than three oxidation events are indicated, these Met residues are dioxidized as demonstrated in the MS/MS spectrum of the +96 adduct peptide in P107S, where all three Met residues contain two additional oxygen atoms (Figure 5).

**Assessment of Oxidation of Heme-Containing Peptides.** Although the results described above suggest that essentially all of the observed oxidative damage to WT MauG upon reaction with H<sub>2</sub>O<sub>2</sub> is localized to Met108, Met114, and Met116, the sequence coverage in this experiment was not complete. Importantly, the peptides containing the covalently attached *c* hemes were not observed under the conditions used for LC–MS/MS. Therefore, the visible absorbance of the heme peptides was used to detect and isolate them by offline HPLC of control and H<sub>2</sub>O<sub>2</sub>-treated samples (Figure 6A). Two major peaks, albeit at significantly different absorbance intensities, were observed in the chromatogram of trypsin-digested WT MauG monitored at 370 nm, consistent with the presence of two heme-containing peptides. ESI-MS of the first peak yielded

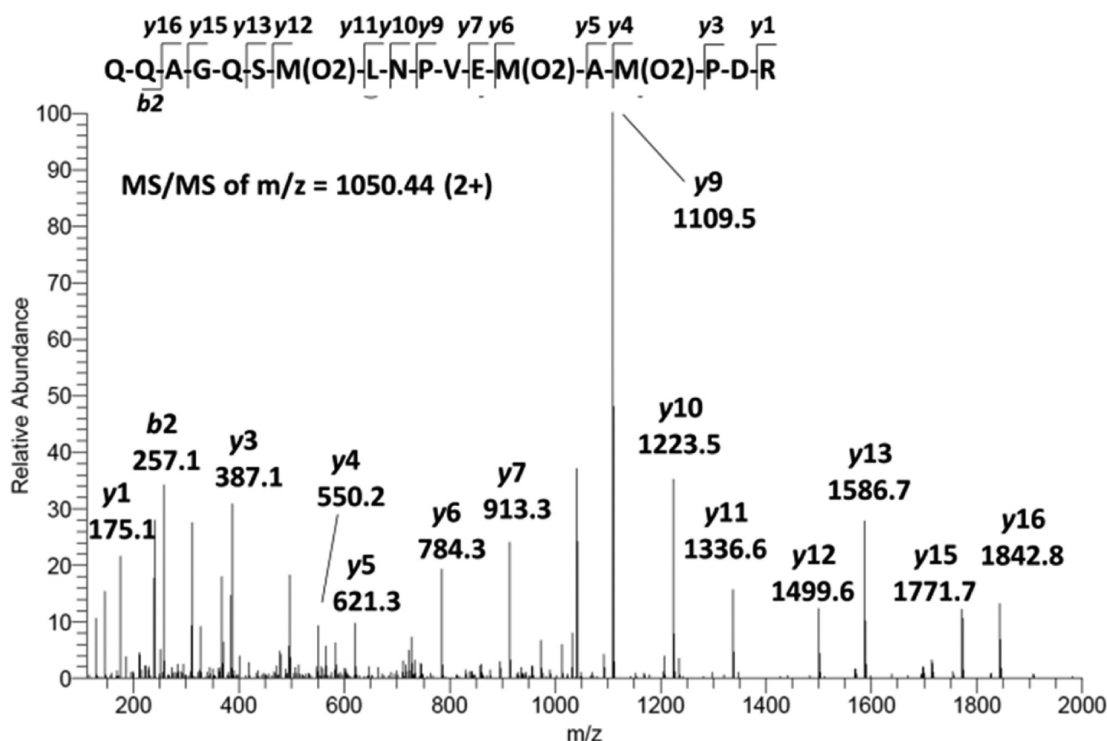


**Figure 5.** MS/MS spectrum of the +2 charge state of the +96 mass of the Q102–R119 peptide obtained by incubation of P107S MauG with a 10-fold excess of  $H_2O_2$ . The monoisotopic  $[M + 2H]^{2+}$  observed precursor  $m/z$  value was 1050.44. The identified y and b ions are mapped onto the primary sequence and demonstrate dioxidation of all Met residues.

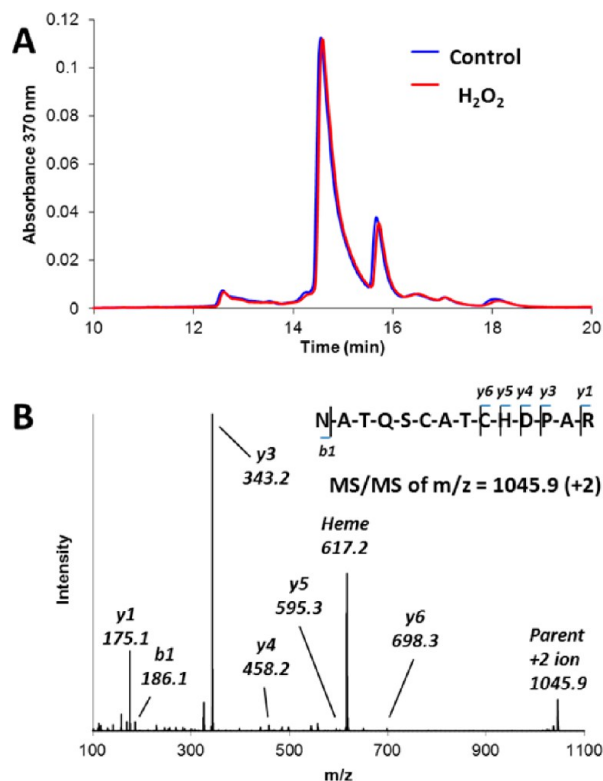


**Figure 6.** (A) HPLC chromatogram of trypsin digests of WT MauG before (blue) and after (red) incubation with a 10-fold excess of  $H_2O_2$  monitored at 370 nm. (B) MS/MS spectrum of the +2 charge state of the high-spin heme-containing peptide. The monoisotopic  $[M + 2H]^{2+}$  observed precursor  $m/z$  value was 1045.9. The identified y and b ions are mapped onto the primary sequence.

a strong signal with a mass consistent with the tryptic peptide bearing the high-spin heme (N26–R39, 2089.8 Da). MS/MS of this species confirmed this assignment and further showed that the heme cofactor is liberated upon fragmentation, yielding a peak for the +1 ion at  $m/z$  617.2 (Figure 6B). There were no mass changes observed for this peptide or its fragments in the sample treated with excess  $H_2O_2$ .

Analysis of the second heme peak is problematic, as a trypsin cleavage site exists within the low-spin c heme binding motif CRLCH. Thus, several masses are possible depending upon whether trypsin can cleave at this site and whether the c heme remains covalently bound bridging the resulting peptides. In our analysis, no masses that could be unambiguously assigned to the low-spin heme-containing peptide were identified. Unfortunately, this peptide also contains Trp199, a key residue in the catalytic radical hopping pathway and a potential site for oxidation. However, the elution profiles for both peaks were completely unchanged in protein samples treated with  $H_2O_2$  (Figure 6A). Oxidation would be expected to alter the elution time relative to that of the unmodified form. Thus, these results suggest that the heme-containing peptides are not sites of significant oxidative modification during reaction of MauG with  $H_2O_2$  in the absence of substrate.

## DISCUSSION

The results presented here show that of the seven Met residues in the MauG sequence (Figure 7A), those at positions 108, 114, and 116 are preferentially oxidized during cycles of bis-Fe(IV) formation and decay in the absence of substrate. These oxidation events correlate with a loss of the ability to form the bis-Fe(IV) intermediate and, consequently, catalytic activity. Mutations to high-spin heme distal residues Glu113 and Pro107 had opposing effects on the susceptibility of MauG to



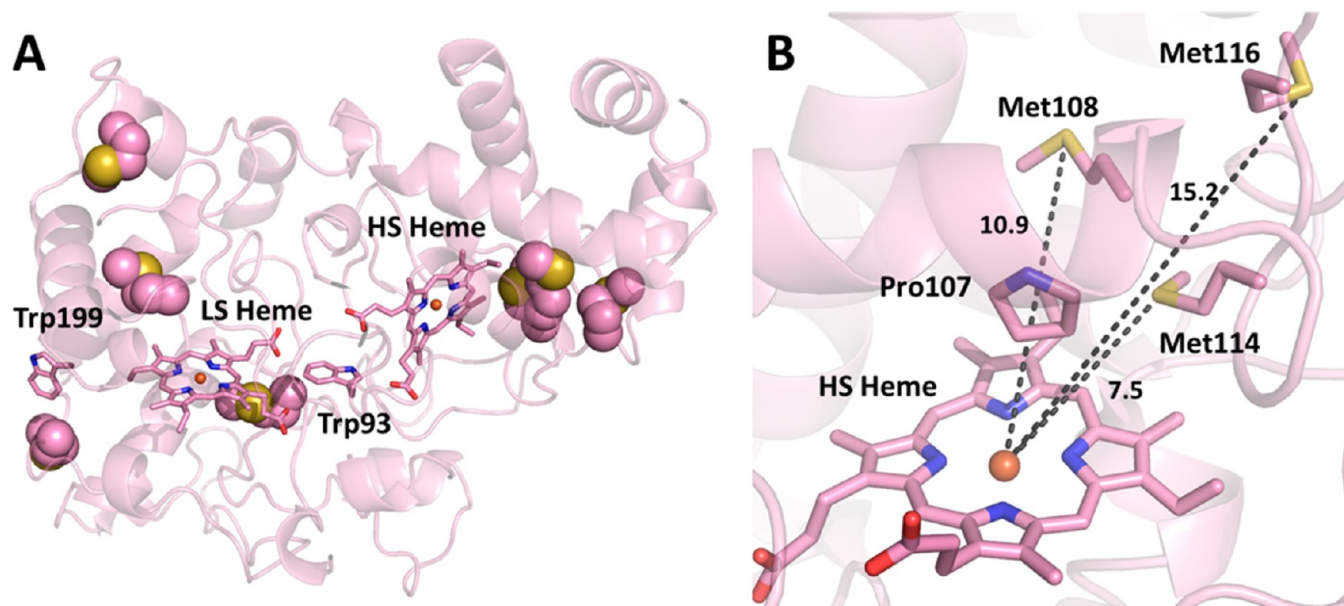


**Figure 7.** (A) Structure of WT MauG in the crystal structure of the WT MauG–preMADH complex (Protein Data Bank entry 3L4M)<sup>23</sup> showing the positions of Met residues (spheres), catalytically important Trp residues, and hemes (sticks). (B) High-spin heme environment of WT MauG showing distances between Met sulfur atoms and the heme Fe. This figure was generated using PyMOL (<http://www.pymol.org>).

oxidation. Specifically, while we observed no significant oxidation of E113Q MauG treated with excess  $\text{H}_2\text{O}_2$ , P107V and P107S MauG exhibited a hyperoxidation phenotype in which Met108, Met114, and Met116 are all oxidized to a greater degree than in the WT protein. Because the peptide containing Trp199 was not observed by mass spectrometry, we cannot conclusively rule out oxidation of this residue during  $\text{H}_2\text{O}_2$ -induced deactivation of WT MauG. However, several pieces of indirect evidence suggest that it is not significantly oxidized in  $\text{H}_2\text{O}_2$ -treated samples. (1) The extent of oxidation in whole protein mass spectra of WT MauG correlates closely with the extent of oxidation in its Q102–R119 peptide. (2) WT and W199F are oxidized to equivalent degrees, both at the whole protein and Q102–R119 peptide levels. (3) The elution profiles of the heme-containing peptides in WT MauG are completely unchanged by treatment with  $\text{H}_2\text{O}_2$ . Therefore, because the only other oxidative modification identified was minor, nonspecific oxidation of Met333, we concluded that the large majority of oxidative damage to WT, W199F, P107S, and P107V MauG occurs at Met108, Met114, and Met116.

Oxidative modification and loss of  $\text{H}_2\text{O}_2$  reactivity also correlated with a change in the UV–vis spectrum of the di-Fe(III) state of MauG after suicide inactivation. A similar spectroscopic change was observed after  $\text{H}_2\text{O}_2$  treatment and loss of reactivity in a myoglobin mutant engineered as a model of cytochrome P450.<sup>25</sup> In this case, compound I formed at the heme oxidized a Trp residue engineered into the distal pocket. The oxidized Trp was proposed to form strong hydrogen bond interactions with a heme-coordinated water or hydroxide, yielding a six-coordinate inhibited state. This could be occurring in WT MauG, as well, where oxidized methionine residues could be playing a similar role or potentially even coordinating the heme iron directly. Methionine oxidation is known to cause significant conformational changes,<sup>26</sup> and oxidized Cys was observed to coordinate the heme in P107C MauG.<sup>14</sup>

In the presence of substrate, bis-Fe(IV) MauG rapidly acquires electrons from preMADH during the biosynthesis of

the TTQ cofactor, which occurs via a hole hopping mechanism of electron transfer via MauG Trp199.<sup>11</sup> However, in the absence of substrate, electrons must be acquired from another source. Under these conditions, these results show that susceptible Met residues can slowly reduce bis-Fe(IV) MauG, becoming oxidized themselves in the process. A third source of electrons may be exogenous reductants, such as buffer components or excess  $\text{H}_2\text{O}_2$ , via catalase activity. The latter possibility is supported by the observation that sequential exposure to stoichiometric  $\text{H}_2\text{O}_2$  was significantly more damaging than exposure to a 10-fold excess. No significant catalase activity could be observed by  $\text{O}_2$  evolution under these conditions, but it is possible that the activity is sufficiently slow to prevent detection by this method.

Mapping the oxidation-susceptible Met residues onto the structure of WT MauG in complex with preMADH<sup>23</sup> shows that they are clustered in a loop above the distal side of the high-spin heme (Figure 7B). Oxidation could occur by direct insertion of an O atom from the high-valent intermediate as is observed for thioether sulfoxidation mediated by cytochrome P450 compound I.<sup>27</sup> However, the sulfur atom of Met108, the residue most sensitive to oxidation, is nearly 11 Å from the heme iron in the crystal structure, making this mechanism unlikely unless the loop is significantly disordered in solution. Perhaps a more likely alternative is that ancillary electron transfer routes terminating in the oxidation of susceptible Met residues may be used when the biosynthetic pathway to preMADH is not available (i.e., in the absence of substrate). In this case, the oxygen atoms introduced in oxidized Met derivatives would most likely derive from solvent water. Thus, we can consider the properties of WT, P107S, and P107V MauG in terms of three possible pathways for reduction of the bis-Fe(IV) intermediate: (1) the biosynthetic electron transfer pathway from preMADH, (2) the ancillary electron transfer pathway(s) from Met108, Met114, and Met116, and (3) the direct reduction pathway by exogenous electron donors. Mutations of Pro107 seem to enhance pathway 2 relative to the others, resulting in an increased level of oxidation in the

absence of preMADH and decreased catalytic efficiency in its presence. Specifically, P107V MauG exhibits a relatively moderate increase in oxidation sensitivity and a ~40% reduction in catalytic activity. P107S MauG exhibits a severe increase in oxidation sensitivity and has no measurable activity toward preMADH. P107C MauG similarly exhibits no catalytic activity, and oxidation of the introduced Cys to Cys sulfinic acid was observed even without exogenous H<sub>2</sub>O<sub>2</sub> treatment, oxidation apparently having occurred during protein expression or purification.<sup>14</sup>

The observation that Met108 is the residue most susceptible to oxidation is intriguing in that it is not the Met residue closest to the heme (Figure 7B). In fact, Met114 is significantly closer. However, Met108 is sequentially adjacent to Pro107, which is very close to the high-spin heme iron with a Fe–C $\gamma$  distance of 4.3 Å. This suggests that a through-bond electron transfer pathway may exist from Met108 through Pro107 to the heme that is more efficient than the shorter, through-space pathway from Met114 or the longer route from Met116. As such, the identity and reactivity of the residue at position 107 will have a significant impact on the efficiency of electron transfer through these ancillary pathways. In addition, mutation of the rigid Pro107 seems to increase the flexibility of the distal heme environment, resulting in coordination of the heme Fe by Glu113 in the P107S mutant, and an increased level of disorder of nearby loops in both P107S and P107V structures.<sup>14</sup> This increased flexibility may allow susceptible residues to more closely approach the heme, enhancing the rate of their oxidation such that it effectively competes with the biosynthetic electron transfer pathway. It may also change the relative susceptibility of each residue to oxidation, as is observed in the Pro107 mutants in which Met116 is oxidized prior to Met114 in contrast to the case for the WT enzyme.

Although the explanation given above adequately describes the effect of Pro107 mutations, it is almost certainly an oversimplification. Mutations to residues in the distal pocket alter the electronic as well as structural properties of the heme environment. For example, the E113Q mutation disrupts redox communication between hemes and alters the distribution of high-valent resonance structures in the H<sub>2</sub>O<sub>2</sub>-oxidized state.<sup>16</sup> These changes resulted in a mutant that could not oxidize either preMADH or its own Met residues. Similarly, Pro107 mutations may alter the nature of the MauG high-valent intermediate in addition to the preferred pathway for electron transfer to that intermediate. Thus, a complete description of these mutants needs to take into consideration the rates of formation and decay of their high-valent species.

The observed charge resonance of bis-Fe(IV) MauG involving both hemes and the intervening Trp93 provides an elegant electronic mechanism of stabilization for this species.<sup>9</sup> However, this alone cannot account for its remarkable stability, as there must be structural elements that prevent the unwanted reaction of the high-valent species with protein residues. This study demonstrates that the rigid proline residue at position 107 near the highly reactive Fe(IV)=O moiety of bis-Fe(IV) MauG limits the oxidation of distal Met residues through ancillary electron transfer routes, which become significant only when the biosynthetic pathway is unavailable or Pro107 is mutated. This structural property, in conjunction with charge resonance stabilization between MauG hemes, provides an efficient means of controlling the potent oxidizing potential of bis-Fe(IV) MauG and helps to explain its remarkable stability in both electronic and structural terms.

Finally, as Met residues are highly susceptible to oxidative modification, it is perhaps counterintuitive that evolution would place three of them in the proximity of the reactive heme of MauG. It has been suggested that methionine may play a protective role in some enzymes by being selectively oxidized by ROS, sparing catalytic activity.<sup>28,29</sup> Clearly, the roles of Met108, Met114, and Met116 are not protective in MauG as activity is lost upon their oxidation. However, this process may protect other proteins and cellular structures by preventing the formation of additional ROS by MauG in the absence of preMADH. The potential biological importance of the deactivation process for MauG is highlighted by the fact that confirmed MauG homologues are rich in Met residues in the distal heme region (residues 106–118, *P. denitrificans* numbering) and Met114 in particular appears to be absolutely conserved. Thus, oxidation of MauG Met residues in the absence of preMADH may provide a convenient means of eliminating this potential source of ROS when MauG activity is not required for TTQ biosynthesis.

## ■ ASSOCIATED CONTENT

### ● Supporting Information

Figures S1 and S2. This material is available free of charge via the Internet at <http://pubs.acs.org>.

## ■ AUTHOR INFORMATION

### Corresponding Authors

\*Address: MSC 3C, P.O. Box 30001, Las Cruces, NM 88003-8001. E-mail: [etyukl@nmsu.edu](mailto:etyukl@nmsu.edu). Telephone: (575) 646-3176. Fax: (575) 646-2649.

\*Address: 6-155 Jackson Hall, 321 Church St. SE, Minneapolis, MN 55455. E-mail: [wilmo004@umn.edu](mailto:wilmo004@umn.edu). Telephone: (612) 624-2406. Fax: (612) 624-5121.

### Funding

This research was supported by the National Institute of General Medical Sciences of the National Institutes of Health via Grants R37GM41574 (V.L.D.), R01GM66569 (C.M.W.), and F32GM97779 (E.T.Y.) and Minnesota Partnership for Biotechnology and Medical Genomics Grant SPAP-05-0013-P-FY06 (C.M.W.).

### Notes

The authors declare no competing financial interest.

## ■ ACKNOWLEDGMENTS

The authors recognize the Center for Mass Spectrometry and Proteomics at the University of Minnesota and various supporting agencies, including the National Science Foundation for Major Research Instrumentation Grants 9871237 and NSF-DBI-0215759 used to purchase the instruments described in this study. Supporting agencies are listed at <http://www.cbs.umn.edu/msp/about>.

## ■ ABBREVIATIONS

MADH, methylamine dehydrogenase; TTQ, tryptophan tryptophylquinone; preMADH, precursor of MADH with incompletely synthesized TTQ; bis-Fe(IV) MauG, redox state of MauG with one heme as Fe(IV)=O and the other as Fe(IV); WT, wild-type; ROS, reactive oxygen species; ESI-MS, electrospray ionization mass spectrometry; LC-MS/MS, liquid chromatography with tandem mass spectrometry; NIR, near-infrared.



## REFERENCES

- (1) Montellano, P. R. O. (2005) *Cytochrome P450: Structure, Mechanism and Biochemistry*, 3rd ed., Academic/Plenum Press, New York.
- (2) Stubbe, J., and van der Donk, W. A. (1998) Protein radicals in enzyme catalysis. *Chem. Rev.* 98, 705–762.
- (3) Warren, J. J., Ener, M. E., Vlcek, A., Jr., Winkler, J. R., and Gray, H. B. (2012) Electron hopping through proteins. *Coord. Chem. Rev.* 256, 2478–2487.
- (4) Stubbe, J., Nocera, D. G., Yee, C. S., and Chang, M. C. (2003) Radical initiation in the class I ribonucleotide reductase: Long-range proton-coupled electron transfer? *Chem. Rev.* 103, 2167–2201.
- (5) Berlett, B. S., and Stadtman, E. R. (1997) Protein oxidation in aging, disease, and oxidative stress. *J. Biol. Chem.* 272, 20313–20316.
- (6) Pearson, A. R., De la Mora-Rey, T., Graichen, M. E., Wang, Y. T., Jones, L. H., Marimanikkupam, S., Agger, S. A., Grimsrud, P. A., Davidson, V. L., and Wilmot, C. M. (2004) Further insights into quinone cofactor biogenesis: Probing the role of MauG in methylamine dehydrogenase tryptophan tryptophylquinone formation. *Biochemistry* 43, 5494–5502.
- (7) Wang, Y. T., Li, X. H., Jones, L. H., Pearson, A. R., Wilmot, C. M., and Davidson, V. L. (2005) MauG-dependent in vitro biosynthesis of tryptophan tryptophylquinone in methylamine dehydrogenase. *J. Am. Chem. Soc.* 127, 8258–8259.
- (8) Li, X. H., Fu, R., Lee, S. Y., Krebs, C., Davidson, V. L., and Liu, A. M. (2008) A catalytic di-heme bis-Fe(IV) intermediate, alternative to an Fe(IV)=O porphyrin radical. *Proc. Natl. Acad. Sci. U.S.A.* 105, 8597–8600.
- (9) Geng, J., Dornevil, K., Davidson, V. L., and Liu, A. (2013) Tryptophan-mediated charge-resonance stabilization in the bis-Fe(IV) redox state of MauG. *Proc. Natl. Acad. Sci. U.S.A.* 110, 9639–9644.
- (10) Choi, M., Shin, S., and Davidson, V. L. (2012) Characterization of electron tunneling and hole hopping reactions between different forms of MauG and methylamine dehydrogenase within a natural protein complex. *Biochemistry* 51, 6942–6949.
- (11) Tarboush, N. A., Jensen, L. M. R., Yukl, E. T., Geng, J. F., Liu, A. M., Wilmot, C. M., and Davidson, V. L. (2011) Mutagenesis of tryptophan199 suggests that hopping is required for MauG-dependent tryptophan tryptophylquinone biosynthesis. *Proc. Natl. Acad. Sci. U.S.A.* 108, 16956–16961.
- (12) Lee, S., Shin, S., Li, X., and Davidson, V. L. (2009) Kinetic mechanism for the initial steps in MauG-dependent tryptophan tryptophylquinone biosynthesis. *Biochemistry* 48, 2442–2447.
- (13) Shin, S., Lee, S., and Davidson, V. L. (2009) Suicide inactivation of MauG during reaction with O<sub>2</sub> or H<sub>2</sub>O<sub>2</sub> in the absence of its natural protein substrate. *Biochemistry* 48, 10106–10112.
- (14) Feng, M. L., Jensen, L. M. R., Yukl, E. T., Wei, X. X., Liu, A. M., Wilmot, C. M., and Davidson, V. L. (2012) Proline 107 is a major determinant in maintaining the structure of the distal pocket and reactivity of the high-spin heme of MauG. *Biochemistry* 51, 1598–1606.
- (15) Wang, Y., Graichen, M. E., Liu, A., Pearson, A. R., Wilmot, C. M., and Davidson, V. L. (2003) MauG, a novel di-heme protein required for tryptophan tryptophylquinone biogenesis. *Biochemistry* 42, 7318–7325.
- (16) Abu Tarboush, N., Yukl, E. T., Shin, S., Feng, M., Wilmot, C. M., and Davidson, V. L. (2013) Carboxyl group of Glu113 is required for stabilization of the diferrous and bis-Fe(IV) states of MauG. *Biochemistry* 52, 6358–6367.
- (17) Li, X. H., Fu, R., Liu, A. M., and Davidson, V. L. (2008) Kinetic and physical evidence that the di-heme enzyme MauG tightly binds to a biosynthetic precursor of methylamine dehydrogenase with incompletely formed tryptophan tryptophylquinone. *Biochemistry* 47, 2908–2912.
- (18) Hildebraunt, A. G., and Roots, I. (1975) Reduced nicotinamide adenine dinucleotide phosphate (NADPH)-dependent formation and breakdown of hydrogen peroxide during mixed function oxidation reactions in liver microsomes. *Arch. Biochem. Biophys.* 171, 385–397.
- (19) Rappsilber, J., Ishihama, Y., and Mann, M. (2003) Stop and go extraction tips for matrix-assisted laser desorption/ionization, nano-electrospray, and LC/MS sample pretreatment in proteomics. *Anal. Chem.* 75, 663–670.
- (20) Lin-Moshier, Y., Sebastian, P. J., Higgins, L., Sampson, N. D., Hewitt, J. E., and Marchant, J. S. (2013) Re-evaluation of the role of calcium homeostasis endoplasmic reticulum protein (CHERP) in cellular calcium signaling. *J. Biol. Chem.* 288, 355–367.
- (21) Shilov, I. V., Seymour, S. L., Patel, A. A., Loboda, A., Tang, W. H., Keating, S. P., Hunter, C. L., Nuwaysir, L. M., and Schaeffer, D. A. (2007) The Paragon Algorithm, a next generation search engine that uses sequence temperature values and feature probabilities to identify peptides from tandem mass spectra. *Mol. Cell. Proteomics* 6, 1638–1655.
- (22) Tang, W. H., Shilov, I. V., and Seymour, S. L. (2008) Nonlinear fitting method for determining local false discovery rates from decoy database searches. *J. Proteome Res.* 7, 3661–3667.
- (23) Jensen, L. M. R., Sanishvili, R., Davidson, V. L., and Wilmot, C. M. (2010) In crystallo posttranslational modification within a MauG/pre-methylamine dehydrogenase complex. *Science* 327, 1392–1394.
- (24) Yukl, E. T., Goblirsch, B. R., Davidson, V. L., and Wilmot, C. M. (2011) Crystal structures of CO and NO adducts of MauG in complex with pre-methylamine dehydrogenase: Implications for the mechanism of dioxygen activation. *Biochemistry* 50, 2931–2938.
- (25) Pfister, T. D., Ohki, T., Ueno, T., Hara, I., Adachi, S., Makino, Y., Ueyama, N., Lu, Y., and Watanabe, Y. (2005) Monooxygenation of an aromatic ring by F43W/H64D/V68I myoglobin mutant and hydrogen peroxide. Myoglobin mutants as a model for P450 hydroxylation chemistry. *J. Biol. Chem.* 280, 12858–12866.
- (26) Dado, G. P., and Gellman, S. H. (1993) Redox control of secondary structure in a designed peptide. *J. Am. Chem. Soc.* 115, 12609–12610.
- (27) Li, C., Zhang, L., Zhang, C., Hirao, H., Wu, W., and Shaik, S. (2007) Which oxidant is really responsible for sulfur oxidation by cytochrome P450? *Angew. Chem., Int. Ed.* 46, 8168–8170.
- (28) Levine, R. L., Mosoni, L., Berlett, B. S., and Stadtman, E. R. (1996) Methionine residues as endogenous antioxidants in proteins. *Proc. Natl. Acad. Sci. U.S.A.* 93, 15036–15040.
- (29) Reddy, V. Y., Desorchers, P. E., Pizzo, S. V., Gonias, S. L., Sahakian, J. A., Levine, R. L., and Weiss, S. J. (1994) Oxidative dissociation of human  $\alpha$ 2-macroglobulin tetramers into dysfunctional dimers. *J. Biol. Chem.* 269, 4683–4691.